Accepted Manuscript

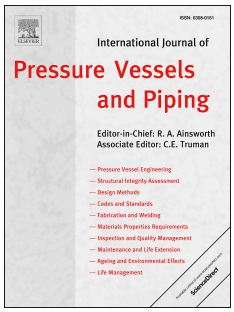

Burst pressure of super duplex stainless steel pipes subject to combined axial tension, internal pressure and elevated temperature

B.A. Lasebikan, A.R. Akisanya

PII: S0308-0161(14)00031-3

DOI: 10.1016/j.ijpvp.2014.03.001

Reference: IPVP 3379

To appear in: *International Journal of Pressure Vessels and Piping*

Received Date: 9 August 2013

Revised Date: 27 February 2014

Accepted Date: 4 March 2014

Please cite this article as: Lasebikan BA, Akisanya AR, Burst pressure of super duplex stainless steel pipes subject to combined axial tension, internal pressure and elevated temperature, *International Journal of Pressure Vessels and Piping* (2014), doi: 10.1016/j.ijpvp.2014.03.001.

BURST PRESSURE OF SUPER DUPLEX STAINLESS STEEL PIPES SUBJECT TO COMBINED AXIAL TENSION, INTERNAL PRESSURE AND ELEVATED TEMPERATURE

B. A. Lasebikan and A. R. Akisanya[1]

School of Engineering,

University of Aberdeen,

Aberdeen AB24 3UE, U.K.

ABSTRACT

The burst pressure of super duplex stainless steel pipe is measured under combined internal pressure, external axial tension and elevated temperature up to 160 ^{o}C. The experimental results are compared with existing burst pressure prediction models. Existing models are found to provide reasonable estimate of the burst pressure at room temperature but significantly over estimate the burst pressure at elevated temperature. Increasing externally applied axial stress and elevated temperature reduces the pressure capacity.

Keywords:

Super duplex stainless steel, mini pipe, uniaxial tensile properties, burst pressure, rupture, failure envelope, temperature effects.

1 INTRODUCTION

An understanding of the burst pressure of pipes and pressure vessels is of particular importance to the oil and gas, chemical and nuclear industry. Consequently the determination of the burst pressure of tubulars has been examined over the years by many researchers. Law and Bowie [1] provided a summary of existing burst pressure prediction models and compared the accuracy of the models with test results on some API X grade steel used in oil and gas production system. Many of the existing models are

[1] Corresponding author. Email: a.r.akisanya@abdn.ac.uk. Fax +44 1224 272497

for tubulars subjected to only internal pressure, with very few incorporating the effect of external axial force on burst pressure.

Production tubulars in oil and gas wells and subsea pipelines are, in general, subjected, in service, to a combination of internal pressure, external pressure, external axial force and elevated temperature. The failure mechanism of a tubular subject to a combination of internal pressure and axial load can be different from that subject to just internal pressure [2]. For example, a tubular without any pre-existing cracks or defects and subject to internal pressure and external axial tension can fail by burst (i.e. rupture) or necking depending on the relative pressure to external axial stress. In order to improve the design and ensure better selection of materials, there is a need for detailed evaluation of burst pressure in the presence of axial stress and elevated temperature.

The analysis of the deformation and failure of metal tubes under combined axial tension and internal pressure is provided in [3- 5] and a detailed analysis of the rupture and necking of tubulars is provided by Klever [2], Stewart et al. [6] and Paslay et al. [7]. None of these analyses include the effect of elevated temperature.

With increasing discovery of new oil and gas fields in high pressure – high temperature and corrosive environment, super duplex stainless steel is a suitable material for the transportation of the hydrocarbon due to its better corrosion resistance in comparison to low-alloy carbon steel. In the present paper, the burst pressure of super duplex stainless steel pipe subject to a combination internal pressure, external axial tension and elevated temperature is examined. Experimental tests are conducted using a mini-pipe, which has been shown to produce reliable and accurate result and to be a cost effective alternative to burst tests on full-size pipes [8]. The experimentally determined failure envelope is compared with predictions by existing theoretical models.

1.1 Burst pressure estimates of tubulars under combined loading

Various burst pressure models exist in literature. Law and Bowie [1] have provided a summary of some of the models for tubulars subject to only internal pressure. Experimental results for pipes made from steel grades with high tensile to yield strength ratio shows that only a few of the models are reliable in predicting the burst pressure. A summary of some of the relevant burst pressure equations for tubulars subject to only internal pressure loading as well as for tubulars subject to combined internal pressure and external axial stress is provided.

Consider a circular cylindrical pipe with inner diameter D_i, outer diameter D_o, wall thickness t and subject to a combined internal pressure P_i, and external axial stress σ_a. We assume pipe has closed ends, the wall thickness is much less than the diameter for thin-walled conditions to hold, i.e. $D_i/t > 20$, and that the tubular is made from a material with uniaxial 0.2% offset yield stress σ_Y and tensile strength σ_{uts}. The burst equations are sometimes expressed in terms of the mean diameter, $D_m = 0.5(D_i + D_o)$. Hereafter, the term burst and rupture are used synonymously.

2.1 Burst pressure equation for pipes subject to only internal pressure

For a close-ended pipe made from an elastic/ideally-plastic material obeying von Mises yield criterion, Hill [3] proposed the burst pressure

$$P_{b,1} = \frac{2}{\sqrt{3}}\sigma_Y \ln\left(\frac{D_o}{D_i}\right), \tag{1}$$

while pipeline design code by DNV [9] gave the burst equation as

$$P_{b,2} = \frac{2}{\sqrt{3}}\frac{2t}{D_m}\sigma_Y \tag{2}$$

which, surprisingly, is widely used in the design of subsea pipelines for assessing the pressure capacity. In fact, neither of these equations actually defines the burst pressure: eq. (1) is the pressure required for through-wall plastic yielding while eq. (2) is the pressure at the onset of plastic yielding at the pipe's inner wall. However, for a thin-walled pipe made from an ideally-plastic material, once the wall thickness has

completely undergone plastically yielding, the plastic strain increases rapidly with a very small increase in pressure leading to burst. This is why (1) gives a good estimate of burst pressure for thin-walled pipes, but not accurate for thick-walled pipe. In order to correct the anomaly, Nadai [10] suggested the use of tensile strength instead of the yield stress and thus proposed:

$$P_{b,3} = \frac{2}{\sqrt{3}}\sigma_{uts}\ln\left(\frac{D_o}{D_i}\right) \tag{3}$$

The effect of strain hardening is not included in any of the burst equations (1) to (3).

Guided by experimental data on pressure vessels made from Q235-D and 20R mild steel, Faupel [11] proposed a burst pressure equation which incorporates the ratio between the yield stress and the tensile strength:

$$P_{b,4} = \frac{2}{\sqrt{3}}\sigma_Y\left(2-\frac{\sigma_Y}{\sigma_{uts}}\right)\ln\left(\frac{D_o}{D_i}\right) \tag{4}$$

Asser Brabin et al. [12, 13] have suggested a modified version of Faupel's burst equation:

$$P_{b,5} = \frac{2}{\sqrt{3}}\sigma_Y\left\{1+\lambda\left(1-\frac{\sigma_Y}{\sigma_{uts}}\right)\right\}\ln\left(\frac{D_o}{D_i}\right) \tag{5}$$

where λ is a material dependent constant; λ = 0.65 for steel vessels. Both (4) and (5) provide better comparison with experimental data. However, none of the above equations follow from finite strain formulation and do not adequately describe the effect of the work-hardening material response on the burst pressure.

Detailed finite deformation analysis of internally pressurised pipe (without any externally applied axial stress) made from a power-law hardening material with strain hardening index *n*, shows that the burst pressure can be expressed based on Tresca yield criterion by [2, 6, 14]

$$P_{bT} = \frac{1}{2^n}\,p_{ref}\,, \tag{6}$$

and for von Mises yield criterion by [2, 6, 15, 16]

$$P_{bM} = \frac{2}{\left(\sqrt{3}\right)^{n+1}} p_{ref} \tag{7}$$

where subscripts T and M are used to indicate burst equation based on Tresca and von Mises respectively, and p_{ref} is a reference load given by

$$p_{ref} = \frac{2t}{D_m}\sigma_{uts} \tag{8}$$

Comparison of the predicted burst pressure by (6) and (7) with experimentally measured values for API X grade tubulars showed that the von Mises based model over-predicts the burst pressure by about 9% while the Tresca based model (6) under-predicts the burst pressure by about 7% [2]. The average of the two predicted values is therefore recommended as this provides a better correlation between predicted and measured values. The average burst pressure in the absence of externally applied axial stress is [2, 6]

$$P_{bC} = \left[\left(\frac{1}{2}\right)^{n+1} + \left(\frac{1}{\sqrt{3}}\right)^{n+1}\right] p_{ref} \tag{9}$$

None of the above models includes the effect of externally applied axial load on the burst pressure.

2.2 Burst pressure equations for pipes subject to combined internal pressure and external tensile stress

A ductile circular pipe that is subject to only a uniaxial tension without any internal or external pressure, will fail by necking when the externally applied axial stress equals the tensile strength σ_{uts} of the material. Necking is the only possible failure mode when no internal or external pressure is applied, as this is identical to conventional uniaxial tensile test. However, under a combined internal pressure and external axial tension, the pipe can fail either by rupture or necking.

Using a combination of Tresca and von Mises yield criterion together with incremental flow theory, Klever [2] and Stewart et al. [6] determined the combination of loads required for the initiation of either of these failure mechanisms for a pipe with

constrained axial deformation. With the constrained axial deformation, the effective axial stress on the pipe's wall is due to a combined effect of the externally applied stress σ_a and the Poisson's effect of the hoop stress; recall the pipe is thin-walled, so the radial component of stress is negligible. The effective axial stress in a thin-walled pipe first subject to an external axial stress σ_a and subsequently fully axially restrained while an internal pressure P_i is applied is given by

$$\sigma_{eff} = \sigma_a - \frac{P_i D_m}{4t} \tag{10}$$

Combined axial stress and internal pressure loading is normally implemented experimentally following one of two loading paths: (i) an internal pressure P_i which is less than the burst pressure is applied and kept constant while an external axial stress is then applied until failure or (ii) an external axial stress which is less than the material's tensile strength is applied followed by the application of an internal pressure until failure occurs. Necking is controlled by the magnitude of the effective axial stress (10), while burst is controlled by the magnitude on internal pressure.

For case (i) with an applied internal pressure P_i (< P_{bC}), the minimum effective axial stress $\sigma_{eff\,N}$ necessary for the initiation of necking is given by [2, 6]

$$\sigma_{eff\ N} = \sigma_{uts}\sqrt{1-(4^{1-n}-3^{1-n})\frac{3^{1+n}}{4}\left(\frac{P_i}{p_{ref}}\right)^2} \tag{11}$$

where the subscript N denotes parameters associated with failure by necking. Necking will occur before rupture when the applied internal pressure P_i satisfies the relation [2]

$$P_i < \frac{2}{3}\left(\frac{\sqrt{3}}{2}\right)^{1-n} p_{ref} \tag{12}$$

For case (ii) where an external axial tensile stress σ_a is applied while the internal pressure is slowly increased until failure, the minimum internal pressure necessary for rupture is given, assuming von Mises yield criterion, by [2, 6]

$$P_{b,R} = \frac{2}{\left(\sqrt{3}\right)^{n+1}} p_{ref} \sqrt{1 - \frac{4^{1-n} - 1}{3^{1-n}} \left(\frac{\sigma_{eff}}{\sigma_{uts}}\right)^2} \qquad (13)$$

where all the parameters are as defined earlier. The corresponding internal pressure at failure based on Tresca yield criterion is as given in eqn. (6). Eqn. (13) reduces to (7) when $\sigma_{eff} = 0$. Rupture will occur before necking provided the effective axial tension satisfies the relation

$$\sigma_{eff} < \left(\frac{\sqrt{3}}{2}\right)^{1-n} \sigma_{uts} \qquad (14)$$

As von Mises based model over predicts while Tresca under predicts, Klever [2] suggests that the chosen estimate for the burst pressure for a power-law hardening material should be the minimum value predicted by eq. (13) and the average of (13) and (6).

A burst pressure equation incorporating the effect of axial stress for a pipe made from an ideally-plastic material was proposed by Paslay et al. [7]. For an ideally-plastic material, $n = 0$, the burst pressure estimated by (13) when $n = 0$ is 15% greater than the estimate using the equation suggested by Paslay et al. [7].

The analysis by Klever [2] and Stewart et al. [6] summarised above accounts for the finite deformation and strain hardening behaviour of the material as well as the effect of combined loading on the failure of cylindrical pipes. Although the burst pressure predicted by these models agree reasonably well with the existing corresponding experimental measurement at ambient temperature, the suitability of the model for burst pressure prediction at elevated temperature is not yet known.

In this paper we examine the failure of circular cylindrical super duplex stainless steel pipe subject to a combination of internal pressure, external axial tension and elevated temperature. The results of the experimental work are compared with the predicted failure loads by the models described above. The authors are not aware of any published

work in open literature on experimental investigation of the failure of SDSS under combination loading either at ambient or elevated temperature.

3 EXPERIMENTAL PROCEDURES

3.1 Material and specimen preparation

The material considered in this study was a cold-worked Grade 125 super duplex stainless steel (SDSS), with a chemical composition primarily based on 25 wt% chromium, 7 wt% nickel, 3 wt% molybdenum, and 2.6% tungsten. This was obtained in tubular form with 7" (178 mm) outside diameter and 14 mm wall thickness.

Mini pipes were used to investigate the response to axial load, internal pressure and combined axial load and internal pressure. The mini pipes were machined from the SDSS tubular; adequate coolant was applied during all cutting and machining processes. The geometry and dimensions of the mini pipe are shown in Figure 1. The dimensions of the mini pipes were chosen to ensure they can be machined from the available thickness of the parent SDSS pipe and that the theoretical burst pressure is less than the pressure capacity (69 MPa) of available hydraulic pump.

The longitudinal direction of the mini pipe was parallel to that of parent SDSS pipe. The outer and inner diameters were respectively 8 mm and 7.5 mm, with a gauge length of 25 mm. The diameters and wall thickness (t = 0.25 mm) were machined to a tolerance of 0.2 μm or less to ensure repeatability; the dimensions therefore satisfy thin-walled pipe conditions. The ends of the pipes were threaded (M10) with spanner flat for assembly purposes; axial load was applied through the threaded connections. One end of the pipe contains a hole for pressure fluid inlet adaptor coupling while the other end was blanked, see Figure 1. A 2 mm undercut between the threaded ends and the main body of the mini pipe was used to position an O-ring (Viton) seal for connection to the pressure adaptor coupling.

3.2 Testing Procedure

Uniaxial tensile, internal pressure, and combine axial load and internal pressure tests were carried out using the mini pipe shown in Figure 1. Axial tension was applied using a screw-driven testing machine in displacement control and at a crosshead speed of 0.5 mm/min (equivalent to a nominal strain rate of 3.33×10^{-4} s^{-1}) while internal pressure was applied using a hydraulic pump; the pressuring medium was hydraulic oil. Post yield, high temperature strain gauges were attached to the outer surface of the mini pipe in the axial and hoop directions. Two axial strain gauges were positioned diametrically opposite each other and set up so as to eliminate bending strains from the measured axial strain, while two strain gauges were also attached in the hoop direction. Tests were performed at room temperature and at elevated temperatures (90, 110 and 160 ^{o}C) using an environmental chamber with radiant heating. The temperature was measured using a thermocouple attached to the outer surface of the specimen. Axial tension and/or internal pressure, was applied to the mini pipe when the required test temperature has been attained. The pressure was measured using a pressure gauge positioned outside the environmental chamber.

For combined axial load/pressure test, the blanked end of the pipe was connected to the moving crosshead of the test machine, while the open end of the pipe was connected to a pressure pump via a fitting and fixed to the base of the test machine. An axial tension force, $F\ (= \pi D_m t \sigma_a)$ was applied first followed by internal pressure P_i. Here t and D_m are respectively the wall thickness and the mean diameter of the pipe and σ_a is the externally applied axial tensile stress. Although it has been indicated that load path is not a major concern in tubes subjected to combined loading [7, 17], the current test method was based on a load path similar to that experienced by a tubing string in oil and gas well completion, i.e. the axial tension was applied to the mini pipe followed by internal pressure.

Different combinations of externally applied axial tensile stress and internal pressure were used to enumerate the combined stress that eventually led to failure. The applied axial stress for the combined loading was chosen to be lower than the tensile strength of

the material. Prior to the application of the internal pressure, the effective axial stress σ_{eff} = σ_a, see (10). When the internal pressure was subsequently applied, the assembly of the samples and the loading fixture imposed an axial constraint on the pipe; this prevented the axial increase in length associated with the application of the internal pressure to an end-capped pipe. Consequently, for the combined loading the effective axial tensile stress on the pipe decreases with increasing magnitude of the applied pressure as indicated in (10).

The loading path for the combined external axial load and pressure was as follows. The required axial stress was first applied, followed by a small increment of internal pressure (2 MPa was used), this led to a slight decrease in the magnitude of the effective axial stress. The axial load was then increased slightly to the required specified level without changing the applied pressure. The process was repeated (i.e. for an applied axial tension, the internal pressure was applied in small increments of 2 MPa followed by an adjustment of the axial tension to the required level) until the mini pipe burst. Whilst mini pipe tests at room temperature were carried out to establish failure envelope for necking and rupture failure modes, the mini pipe tests at elevated temperature focused only on rupture failure envelope. For elevated temperature tests, the introduction of hydraulic fluid in order to increase the pressure led to a slight decrease in the surface temperature of the specimen. The specimen was allowed to attain the required surface temperature before the next increment in pressure was applied. This process is repeated until the mini pipe burst.

4 Results and Discussion

4.1 Response to uniaxial load without internal pressure

Uniaxial tensile tests were carried out on the mini pipe (without internal pressure) at room temperature to obtain the tensile strength, yield stress and the strain hardening index. Five specimens were tested; all five specimens tested failed by circumferential split post necking at the wall of the pipe. A typical room temperature uniaxial stress – strain response obtained from the mini pipe in the current study is compared in Figure 2 with that from conventional solid circular cylindrical tensile specimen [18]. There is

very little strain hardening and a reasonable agreement was obtained between the uniaxial responses from the two specimen geometries. The low strain hardening is due to the cold working associated with the manufacturing process of the SDSS pipe.

A summary of the room temperature uniaxial material properties for the mini pipe and the conventional tensile specimen geometry is shown in Table 1. The uniaxial loading of the mini pipes resulted in an average 0.2% offset yield stress of 914 MPa at room temperature compared to a value of 969 MPa obtained from conventional uniaxial tensile specimen [18]. This small difference in the average value of the uniaxial yield stress, roughly 6%, is attributable to possible deviation in the mini pipe's nominal wall thickness of 0.25 mm. However, the average values of other properties (i.e. tensile strength, strain hardening index and Young's modulus) obtained from the mini pipe at room temperature are comparable to the corresponding property obtained from the conventional tensile specimen at room temperature. It is noted that the material properties obtained at room temperature using the mini pipe has a much larger standard deviation than those obtained using the conventional tensile specimens. For example, the standard deviation in the measured uniaxial yield stress was 39.5 MPa for the mini pipe and 1.8 MPa for the conventional solid circular cylindrical specimen. Taking the standard deviation into account, it can be assumed that there is no significant difference in the measured properties using the mini pipe and conventional solid circular cylindrical specimen. Consequently no uniaxial axial loading test of the mini pipe was carried out at elevated temperature. As the focus of the study is on the onset of failure, the 0.2% offset yield stress and the tensile strength of the mini pipe at elevated temperature are assumed to be equal to the corresponding properties obtained using the conventional specimen at the same temperature; these were obtained in a separate study [18] using a 5 mm solid circular cylindrical specimen and shown, for completeness, in Table 2.

4.2 Response to internal pressure without external axial load

The end-capped mini pipe was also subjected to internal pressure to failure to establish the burst pressure without externally applied axial tension. There was no constraint on

the axial displacement of the pipe during the internal pressurisation. The internal pressure versus strain for two mini pipe specimens at room temperature is shown in Figure 3; the response at elevated temperature is qualitatively similar to that shown in Figure 3.

Due to the experimental set up and specimen configuration, i.e. closed-end pipe, the internal pressurisation of the pipe resulted in the development of mainly hoop strain with a relatively smaller axial strain (due to Poisson's effect). There was a sudden increase in the hoop strain as the applied pressure got closer to the burst pressure. The measured hoop strain at failure was between range of 0.008 and 0.03 for all the tests. For example, Pipe 1 in Figure 3 failed at a hoop strain of 0.008 while Pipe 2 failed at a strain of 0.025. Using the room temperature uniaxial tensile properties obtained for the mini pipe test geometry (see in Table 2), we predict a failure strain of 0.014 based on the analysis of Klever [2], a strain of 0.029 based on Zhu and Leis [19] and a strain of 0.013 based on the model by Gassler and Vogt [20]. The measured failure hoop strain is therefore in good agreement with predictions by existing models in the literature.

Due to the hoop strain dominance, the pipes failed by burst (Fig. 4). The axial length of the fracture increased with increasing magnitude of the burst pressure. It was noted that the fracture did not run the full length of pipe because the SDSS pipe is a relatively tough material and energy is dissipated as the internal pressure is lost at burst. The resistance of the pipe to fracture propagation is outside the scope of the current study.

The measured average burst pressure was 67.2, 56.1, 54.5 and 45.4 MPa at 22, 90, 110 and 160 ^{o}C, respectively. The burst pressure decreased by about 30% as the temperature increased from 22 to 160 ^{o}C. As shall be discussed later, this reduction in burst pressure at elevated temperature can not be attributed primarily to the decrease in material strength at elevated temperature. These results show for the first time the effect of temperature on the burst pressure of SDSS stainless steel pipes. If this is not adequately accounted for in the design of super duplex stainless steel tubulars used in

high pressure – high temperature environment, it could result in over estimation of burst pressure.

A comparison between the measured burst pressure and predictions using the models described in section 2 is given in Table 3. For the comparison, the uniaxial tensile properties measured using solid circular cylindrical tensile specimens (Tables 1 and 2) are used for the prediction of the burst pressure at ambient and elevated temperatures. The burst pressure predicted at room temperature by Hill's [3] and DNV [9] (eqs. (1) and (2) respectively)without considering the strain hardening is 72.2 MPa; this compares reasonably well with the measured value of 67.2 MPa. The relatively good agreement here is due to the fact that the hardening response of the material is very mild; the strain hardening index is in the range $0.02 \leq n \leq 0.03$, and the thin wall of the mini pipe meant that once plastic deformation starts from the inside surface of the pipe, it quickly spreads to the outer surface leading to rupture with minimum increase in the pressure. Consequently, the models which are based on yield pressure can be used to provide a reasonable estimate for the burst pressure as well provided the wall is sufficiently thin as it is in this particular study.

The predicted value of the burst pressure at room temperature was 72.5 MPa by Klever [2] and Stewart et al. [6] finite deformation based model (9) which incorporates strain hardening. The measured burst pressure is only 7% less than the prediction which incorporates strain hardening deformation. Note that the prediction does not take into consideration geometric variation, i.e. non-uniform wall thickness and diameter along the length of the pipe. With the relatively small nominal wall thickness of the pipe (t = 0.25 mm), a local reduction of the wall thickness to 0.23 mm is sufficient to reduce the measured burst pressure by 7%.

With the use of the elevated temperature properties in calculating the predicted burst pressures, all the existing models significantly over predicts the burst pressure at elevated temperature (Table 3). The difference between measured and predicted burst pressure increased as the temperature increased. For example, for all the models

considered, the difference between the predicted and measured burst pressure was between 15 and 25% at a temperature of 90 ^{o}C while this difference increased to between 30 and 45% at 160 ^{o}C. It is noted that the measured uniaxial yield stress of the solid circular cylindrical tensile specimen was used for determining the predicted burst pressure at ambient and elevated temperatures. Results obtained from previous study [18] and summarised in Table 2 show a 6% reduction in the room temperature average uniaxial yield stress measured using a mini pipe when compared with that measured using a solid circular specimen. Even if this level of difference in the uniaxial axial yield stress is assumed at elevated temperature, the measured burst pressure at elevated temperature is still significantly less than the predictions by the existing models. There is a need for an assessment of the reliability and suitability of these models at elevated temperature.

4.3 Burst pressure under combined internal pressure and axial load

The mini pipes failed by necking when subjected to only axial tension and by rupture when subjected to purely internal pressure. The combined loading tests of the pipes were carried out to determine the effect of the combination of axial tension and internal pressure on the failure mechanism and on the failure envelope. These tests were also carried out at various temperatures: room temperature, 90, 110 and 160 ^{o}C. Once the required axial load was established the pipe was pressurised incrementally while maintaining the required axial tensile stress by adjusting the applied load. A typical evolution of the axial stress, axial strain and hoop strain is shown in Figure 5. When axial tension was applied, the decrease in outside diameter due to Poisson's effect resulted in compressive OD hoop strain (Figure 5b). For an initial external axial stress of about 550 MPa, the hoop strain remained negative until the internal pressure exceeded about 9.3 MPa and hoop strain continues to increase until failure. This trend applies to the rupture failure mechanism only whereas in tests where axial load was dominant i.e. failure due to necking, the hoop strain remained compressive until failure.

The failure mechanism in the combined axial tension and internal pressure in the mini pipe was controlled by the relative magnitude of the applied tensile axial stress and the

internal pressure as given by (12) and (14). When the stress was dominated by the axial tension the mini pipe failed by necking and if the hoop stress due to internal pressure was dominant the mini pipes failed by burst or a longitudinal crack (Figure 4) in the gauge section. These failure mechanisms are not affected by the test temperature.

The measured combination of effective axial stress and internal pressure at failure is shown in Figure 6 for tests carried out at ambient temperature and elevated temperature. The internal pressure at failure decreases as the effective axial stress increases. As the temperature increased, the strength of the material decreased; thus the ability of the mini pipe to withstand combined load diminished.

Klever's [2] model for predicting the combination of internal pressure and axial load required for the failure of oil country tubular goods (OCTG) given in eqns. (11) and (13) is compared with the measured failure envelope in stress space using the corresponding material properties at the test temperature, see Figure 6. The predicted failure envelope compares reasonably well with the experimental results for the range of temperature considered in this study, except for the case of only internal pressurisation where the model estimates a higher burst pressure than the measured value. The effect of temperature on the failure envelope using the theoretical model and measured material properties is illustrated in Figure 7. The axial load capacity decreases with increasing internal pressure and temperature.

5 Conclusions

The combination of internal pressure and axial load required to initiate failure by necking and burst in a 25Cr SDSS pipe has been determined at a range of temperatures using a mini pipe specimen configuration. The measured burst pressure in the absence of externally applied axial stress is in good agreement with the elastic-plastic and perfectly plastic predictions at room temperature. However, existing models significantly over predict the burst pressure at elevated temperature. The failure loads decreased with increasing temperature; this demonstrates the importance of temperature

considerations in design against failure in high pressure – high temperature applications of the SDSS material.

Acknowledgements

The authors acknowledge the assistance of the staff at the Central Workshop, School of Engineering, University of Aberdeen, in relation of machining of the specimens and experimental procedures. In particular, Stuart Herbert, Marcus Goudie Alastair Robertson and James Gall.

References

[1] Law M, Bowie G. Prediction of failure strain and burst pressure of high yield-to-tensile strength ratio linepipe. International Journal of Pressure Vessels and Piping 2007; 84:487-92.

[2] Klever FJ. Formulas for rupture, necking and wrinkling of OCTG under combined loads. SPE Annual Technical Conference and Exhibition, San Antonio, Texas USA, 24-27 September 2006; SPE Paper 102585

[3] Hill R. Mathematical theory of plasticity. New York: Oxford University Press; 1950.

[4] Tomita Y, Shindo A, Nagai M. Axisymmetric deformation of circular elastic-plastic tubes under axial tension and internal pressure. International Journal of Mechanical Sciences 1984; 26:437-444.

[5] Lessells JM, Macgregor CW. Combined stress experiments on a nickel-chrome-molybdenum steel. Journal of the Franklin Institute 1940; 230:163-181.

[6] Stewart G, Klever FJ, Ritchie D. An analytical model to predict the burst capacity of pipelines. Proceedings of the 13th International Conference on Offshore Mechanics and Artic Engineering, OMAE 1994; p177-188 (ISBN: 0791812685).

[7] Paslay PR, Cernocky EP, Wink R. Burst pressure prediction of thin-walled ductile tubulars subjected to axial load. SPE Applied Technology Workshop on Risk Based Design of Well Casing and Tubing, Houston. 1998; SPE 483327.

[8] Cernocky EP, Aaron VD, Paslay PR, Wink RE. Combined axial tension/compression and internal pressure testing of mini-pipe specimens in H_2S environment to determine three dimensional (triaxial) stress states which produce crack initiation failure: explanation of new test fixture, mini-pipe specimen and preliminary test results. SPE High Pressure/High Temperature Sour Well Design Applied Technology Workshop, The Woodlands, Texas, 17-19 May 2005; SPE 92577.

[9] DNV-OS-F101 Offshore Standard. Submarine Pipelines Systems. October 2010.

[10] Nadai A. Plasticity. New York and London: Mcgraw-Hill; 1931.

[11] Faupel JH. Yield and bursting characteristics of heavy-wall cylinders. Transaction of ASME, Journal of Applied Mechanics 1956; 78:1031-64.

[12] Asser Brabin T, Christopher T, Nageswwara Rao B. Investigation of failure behavior of unflawed steel cylindrical pressure vessels using FEA. Multidisciplinary Modelling in Materials and Structures 2009; 5:29-42.

[13] Asser Brabin T, Christopher T, Nageswwara Rao B. Bursting pressure of mild steel cylindrical vessels. International Journal of Pressure Vessels and Piping 2011; 88:119-22.

[14] Zhu X, Leis BN. Theoretical and numerical predictions of cylindrical of bust pressure of pipelines. Transaction of ASME, Journal of Pressure Vessel Technology 2007; 129:644-52.

[15] Subhananda Rao A, Venkata Rao G, Nageswwara Rao B. Effect of long-seam mismatch on the burst pressure of maraging steel rocket motor cases. Engineering Failure Analysis 2005; 12:325-36.

[16] Marin J, Sharma M. Design of thin-walled cylindrical vessel based upon plastic range and considering anisotropy. Welding Research Council Bulletin 1958; 40.

[17] Gao Z, Cai G, Liang L, Lei Y. Limit load solutions of thick-walled cylinders with fully circumferential cracks under combined internal pressure and axial tension. Nuclear Engineering and Design 2008; 238:2155-64.

[18] Lasebikan BA, Akisanya AR, Deans WF. The mechanical behaviour of super duplex stainless steel at elevated temperature. Journal of Materials Engineering and Performance 2013; 22(2):598-606.

[19] Zhu X, Leis BN. Strength criteria and analytic predictions of failure pressure in line pipes. International Journal of Offshore Polar Engineering 2004; 14:125-31.

[20] Gaessler H, Vogt GH. Influence of yield-to-tensile ratio on the safety of pipelines. 3E International, 28 Jahgag, Heft, 3 April 1989; 165-72.

LIST OF TABLE

FIGURE CAPTIONS

Figure 1 The geometry and dimension of the mini pipe. Dimensions are in mm.

Figure 2 Uniaxial stress – strain response for conventional solid circular cylindrical tensile specimen and a mini pipe. Tests were carried out at room temperature and at a nominal strain rate of 3.33×10^{-4} s^{-1}.

Figure 3 Evolution of the hoop and axial strain during internal pressurisation of a close-ended SDSS mini pipe.

Figure 4 Rupture of the mini pipe due to internal pressure.

Figure 5 A typical stress - strain (axial and hoop) evolution for a mini pipe subjected to axial tension (550 MPa) and internal pressure until rupture at 90 ^{o}C.

Figure 6 Failure envelope of the SDSS pipe in the axial stress - internal pressure space (a) Room temperature, (b) 90 ^{o}C, (c) 110 ^{o}C, and (d) 160 ^{o}C.

Figure 7 Predicted failure envelope using the measured material properties.

Table 1: Mechanical properties at room temperature for mini pipe and conventional tensile specimen. The values are average of results from five nominally identical specimens.

Property	**Average Mini Pipe**	**Conventional solid circular tensile specimen [18]**
0.2% offset Yield Stress (MPa)	914 ± 39.5	969 ± 1.8
Tensile Strength (MPa)	1059 ± 27.7	1063 ± 6.3
Young's Modulus (GPa)	209 ± 10.1	208 ± 2.2
Strain hardening index, *n*	0.028	0.027

Table 2: Effect of temperature on the uniaxial mechanical properties of the 25Cr SDSS obtained using conventional solid circular cylindrical rod specimen [18].

Property	**90 °C**	**110 °C**	**160 °C**
0.2% offset Yield Stress, σ_Y, (MPa)	881	851	821
Tensile Strength, σ_{uts} (MPa)	948	935	888
Young's Modulus, E (GPa)	207	201	197
Strain hardening index, n	0.025	0.022	0.030

Table 3: Comparison of measured burst pressure with predictions. Values are in MPa.

	22 °C	**90 °C**	**110 °C**	**160 °C**
Experiment (current study)	67.2	56.1	54.5	45.4
Hill's formulae; eq. (1), Ref. [3]	72.2	65.6	63.4	61.2
DNV ; eq. (2), Ref. [9]	72.2	65.6	63.4	61.2
Nadia's formulae; eq. (3), Ref. [10]	79.1	70.6	69.7	66.1
Faupel's formulae; eq. (4), Ref. [11]	78.6	70.2	69.1	65.8
Asser Brabin's formulae; eq. (5), Ref. [12, 13]	76.3	68.6	67.1	64.2
Klever and Stewart et al.; eq. (9), Ref. [2, 6]	72.5	64.8	64.1	60.6

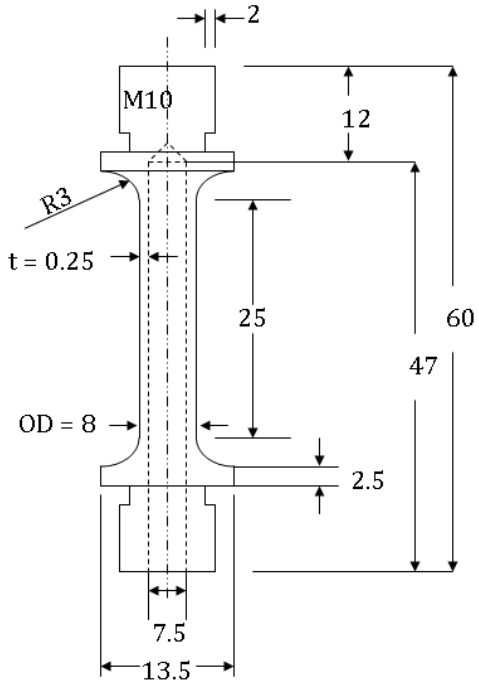

Figure 1

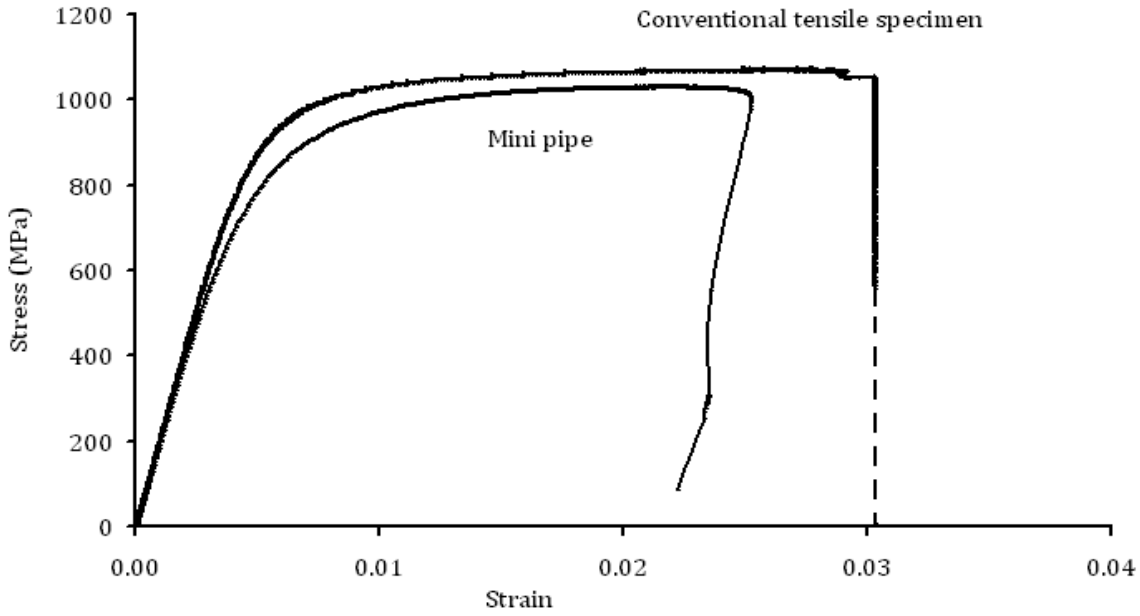

Figure 2

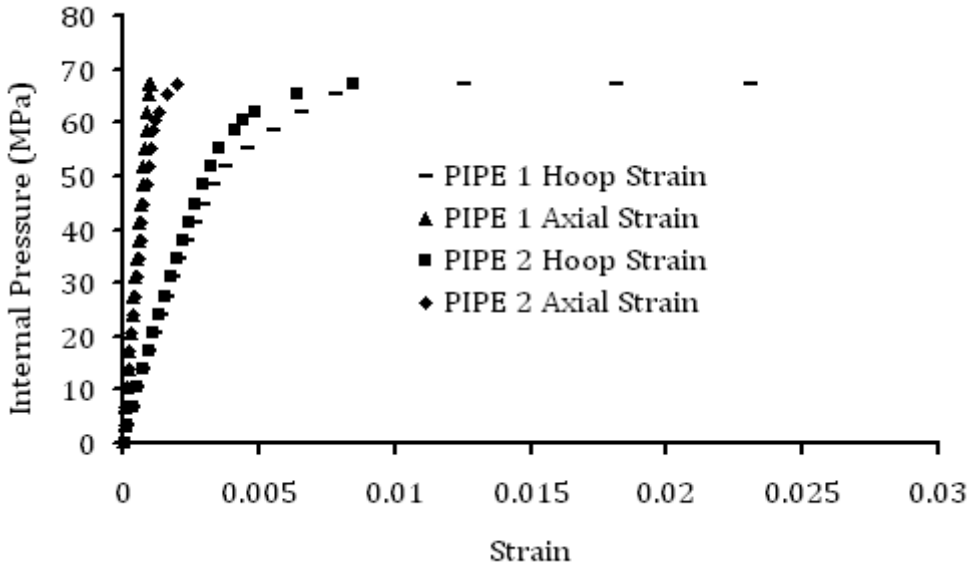

Figure 3

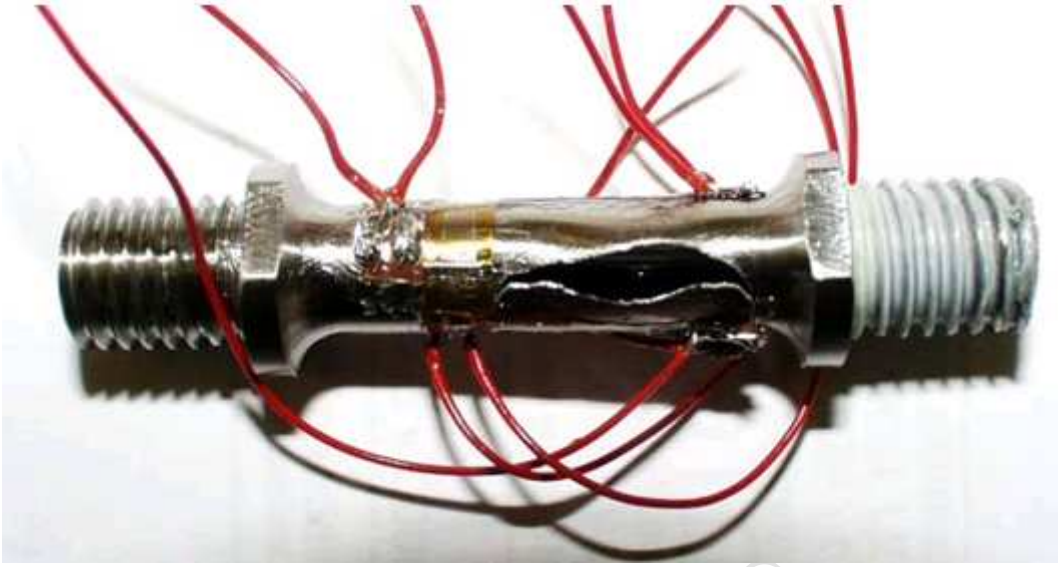

Figure 4

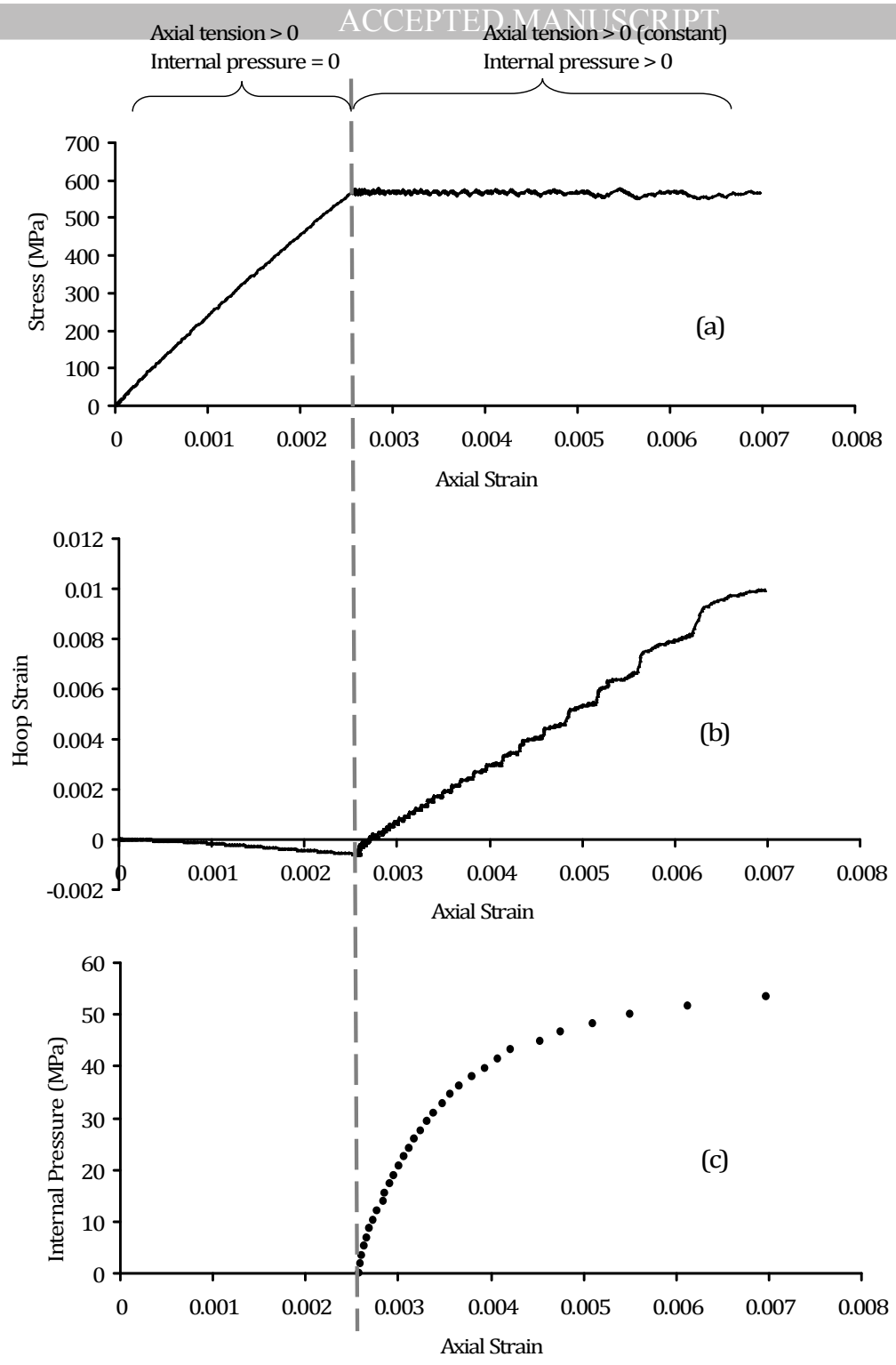

Figure 5

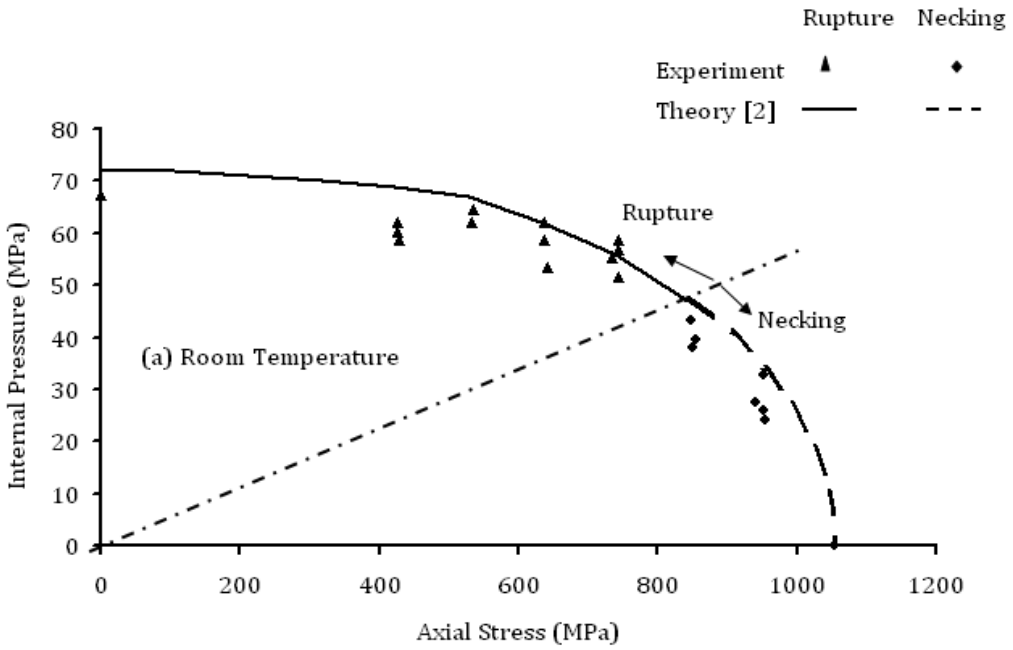
Rupture
Necking
Experiment
Theory [2]
Rupture
Necking
(a) Room Temperature
Internal Pressure (MPa)
Axial Stress (MPa)
0
10
20
30
40
50
60
70
80
0
200
400
600
800
1000
1200

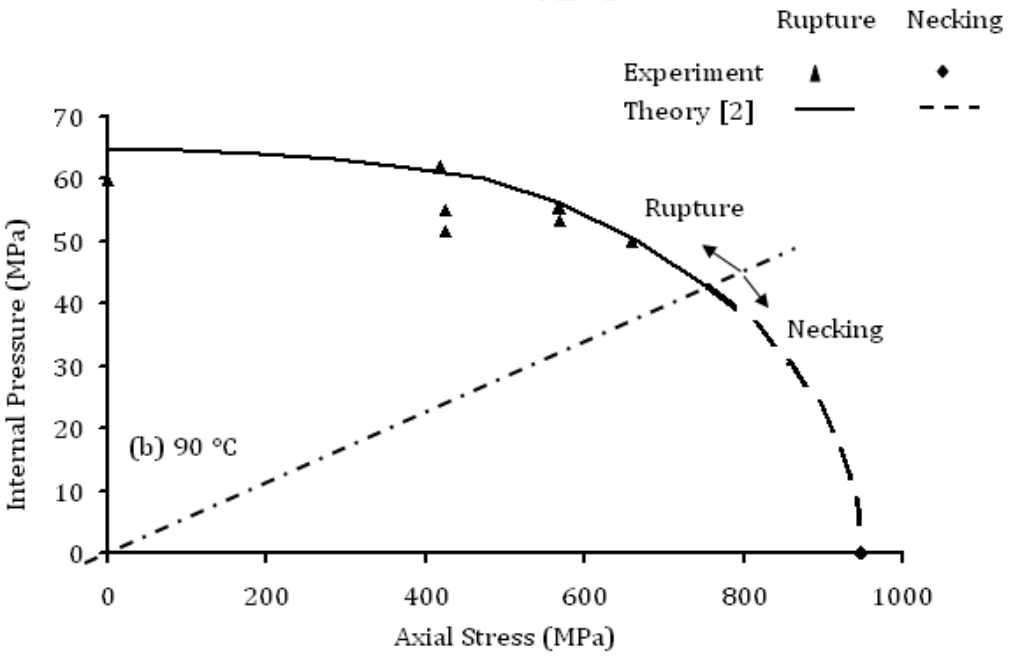
Rupture
Necking
Experiment
Theory [2]
Rupture
Necking
(b) 90 °C
Internal Pressure (MPa)
Axial Stress (MPa)
0
10
20
30
40
50
60
70
0
200
400
600
800
1000

Figure 6 (a & b)

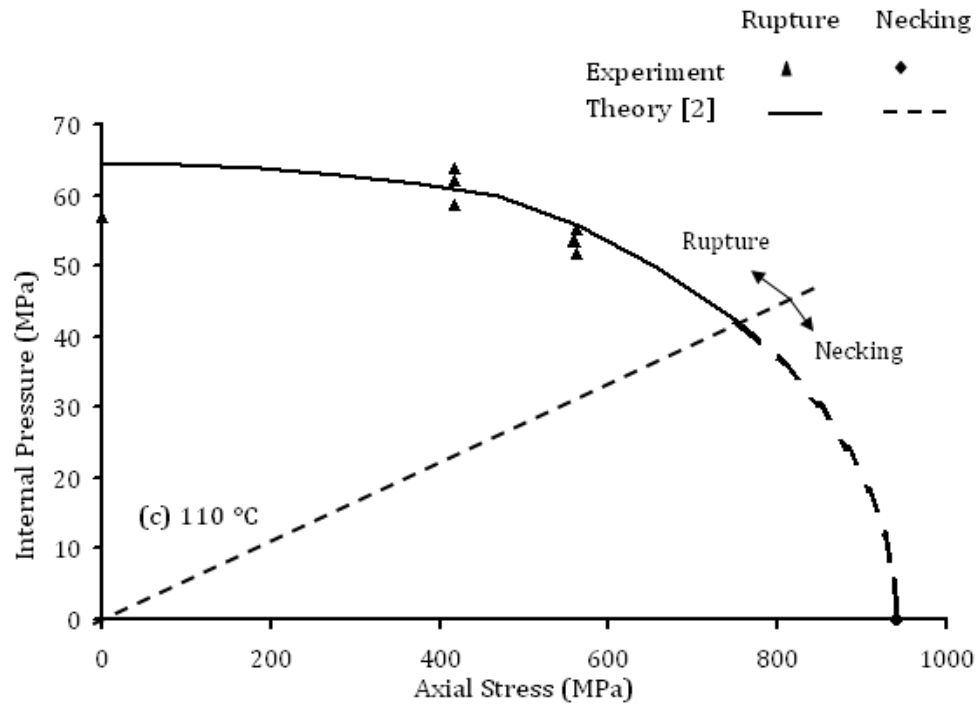
Rupture
Necking
Experiment
Theory [2]
Internal Pressure (MPa)
Axial Stress (MPa)
Rupture
Necking
(c) 110 °C
0
10
20
30
40
50
60
70
0
200
400
600
800
1000

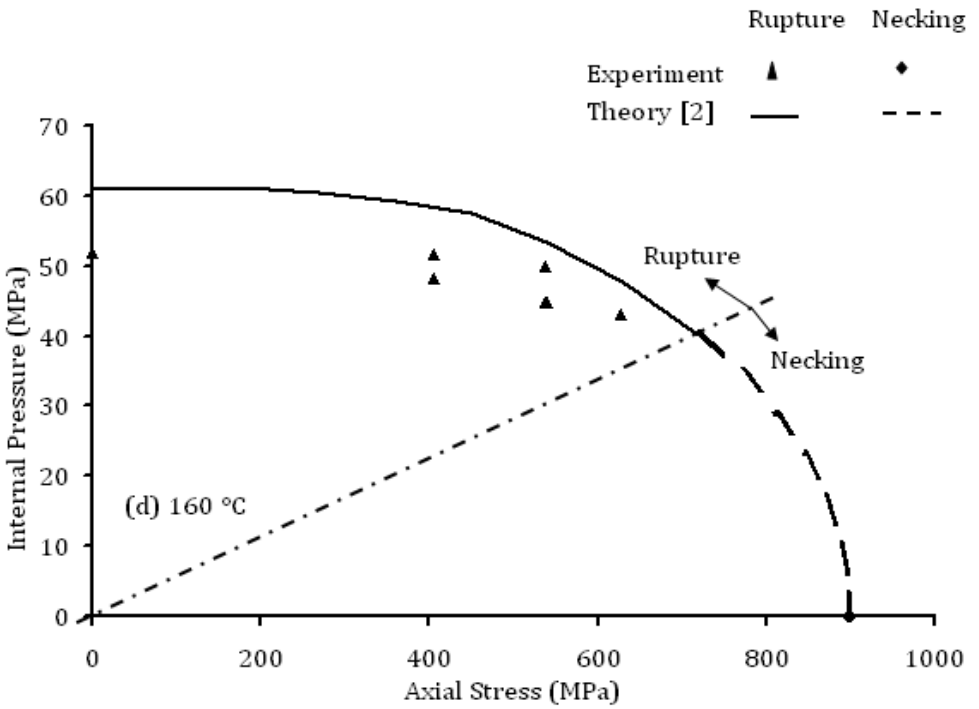
Rupture
Necking
Experiment
Theory [2]
Internal Pressure (MPa)
Axial Stress (MPa)
Rupture
Necking
(d) 160 °C
0
10
20
30
40
50
60
70
0
200
400
600
800
1000

Figure 6 (c & d)

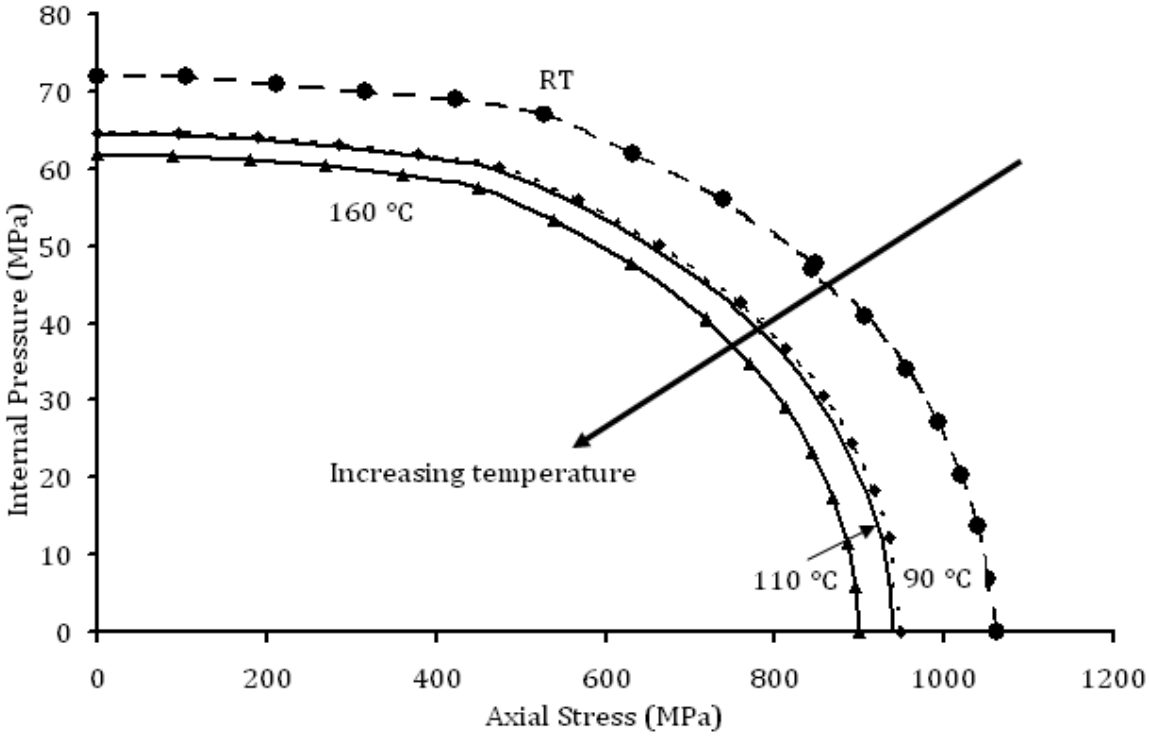

Figure 7

HIGHLIGHTS

- The burst pressure of super duplex steel is measured under combined loading.
- Effect of elevated temperature on burst pressure is determined.
- Burst pressure decreases with increasing temperature.
- Existing models are reliable at room temperature.
- Burst strength at elevated temperature is lower than predictions.